AIAA JOURNAL
Vol. 34, No. 6, June 1996

Simulations of Particle Dynamics in a Confined Shear Flow

E. J. Chang* and K. Kailasanath†
U.S. Naval Research Laboratory, Washington, D.C. 20375

The dynamic behavior of particles injected into the high-speed shear flow in the confined geometry of an axisymmetric dump combustor is studied computationally using the flux-corrected transport algorithm and a Lagrangian approach to track particles in the flow. Small particles are seen to travel with the large vortical structures, while intermediate sized particles are seen to form sheets as they are ejected from these structures. Dispersion of the particles is found to be optimal at Stokes numbers on the order of unity when particles that have been deposited on the combustor walls are neglected. Further analysis shows that it is the shedding frequency that governs the dispersion, even at downstream locations where the first merging frequency governs the fluid flow. This property is observed for all particle sizes studied except for cases at very low Stokes numbers, where the merging frequency, as well as the frequency obtained by combining the merging and shedding frequencies, is observed. A correlation between particle size and flow vorticity is also obtained and shows that high concentrations of particles can be associated with high vorticity for small particles, whereas the opposite is true for intermediate to large sized particles.

Introduction

MULTIPHASE flows are encountered in many practical combustion applications. In many systems, liquid fuel is sprayed into the combustor, where it mixes and burns with the air. In some newer applications such as the combustion of high-energy fuels, the fuel may actually be injected in the form of a slurry or as solid particles in a gaseous stream. Therefore, there is a critical need to study the dynamics of particles in shear flows such as those encountered in propulsion systems.

There has been much work done in the past regarding the behavior of particles in fluid flows. Much of this work has focused on either idealized flows with no confining boundaries such as homogeneous isotropic turbulence[1,2] and free shear layers[3,4] or on specific problems such as particle deposition and reflection in boundary layers near walls.[5,6] Some work has also been done involving heavy particles injected into freejets.[7,8] However, little basic work has been done in areas with true engineering applications. In general, in practical applications, fuel–air mixing and combustion take place in confined geometries. A shear layer in such a confined system can be significantly different from a free shear layer because of the interactions between the acoustics of the confined system and the large-scale vortical structures in the shear layers.[9] In addition, the confinement could significantly inhibit the dispersion and migration of particles. This paper reports on a numerical study of the behavior of particles injected into a high speed shear layer such as that encountered in the dump combustor of a ramjet system.

Previous work dealing with heavy particles includes that of Wang and Maxey[2] for particles settling as the result of gravity in homogeneous isotropic turbulence. They found that sheets of particles form leading to increased settling rates when the particle response time is on the order of the Kolmogorov scale. Such sheets, formed in the braid region between vortex structures, have also been observed in the experiments of Longmire and Eaton[8] for a particle laden round jet as well as in the numerical work of Martin and Meiburg,[10] who found the existence of particle sheets in a free shear layer, here at Stokes number $S \approx 1$, leading to preferential particle dispersion at Stokes numbers on the order of unity.

Crowe et al.[11] investigated heavy particle behavior in a turbulent free shear flow. They found that intermediate sized particles, with response times on the order of the observed characteristic flow time, were quite strongly dispersed, in some cases to an extent greater than that of the fluid, by large-scale coherent flow structures. In addition, they found that small particles tended to follow fluid elements, whereas for larger sized particles, the flow had little influence on particle trajectory. The experimental work of Lázaro and Lasheras[4,12,13] confirms the existence of optimal dispersion in a plane turbulent mixing layer for intermediate sized particles and further demonstrates the selective dispersion of different sized particles. For the unforced case, dispersion was always found to be less than the fluid momentum, whereas in the forced case it was possible for particle dispersion to exceed that of the fluid momentum.

Similarly, for heavy particles injected into axisymmetric jets Chung and Troutt[14] have demonstrated optimal dispersion for intermediate sized particles. More recently, this result has also been observed by Uthuppan et al.,[7] who found enhanced dispersion of intermediate size particles in an axisymmetric jet and explored different mechanisms responsible for the observed dispersion. Reviews of these and other results concerning particle dispersion in shear flows can be found in Crowe et al.[15] and Eaton and Fessler.[16]

One of the issues investigated here is whether dispersion will still be maximized in a flow with confining boundaries, such as the ramjet combustor, at Stokes numbers on the order of unity. We will also examine the relationship between particle dispersion and vortex shedding and merging as well as the relationship between flow vorticity and particle concentration.

Numerical Model

Simulation of Fluid Flow

The flow into a central dump ramjet combustor is computed by solving the compressible, time-dependent, conservative equations for mass, momentum, and energy in an axisymmetric geometry using the flux-corrected transport (FCT) algorithm,[17] a conservative, monotonic algorithm with fourth-order phase accuracy. No explicit term representing physical viscosity is included in the model. No artificial viscosity is needed to stabilize the algorithm because of the residual numerical diffusion present that effectively behaves like a viscosity term for short wavelength modes on the order of the zone size. This damping of the short wavelengths is nonlinear, and the effects of the residual viscosity diminish very quickly for long wavelength modes, resulting in a high effective Reynolds number. This approach called monotonically integrated large-eddy simulation is described in detail elsewhere.[18] This is the same approach used by Kailasanath et al.[9,19–21] in previous simulations of ramjet combustor flows.

A schematic of the idealized ramjet used is shown in Fig. 1. This particular configuration was chosen because of the extensive studies[9,19–22] of nonreactive and reactive flows performed on this

Presented as Paper 95-0812 at the AIAA 33rd Aerospace Sciences Meeting, Reno, NV, Jan. 9–12, 1995; received Feb. 28, 1995; revision received Jan. 22, 1996; accepted for publication Feb. 16, 1996.

*Mathematician, Center for Reactive Flow and Dynamical Systems, Laboratory for Computational Physics and Fluid Dynamics.

†Head, Center for Reactive Flow and Dynamical Systems, Laboratory for Computational Physics and Fluid Dynamics.

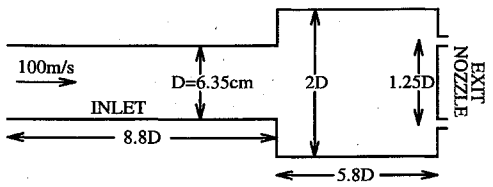

Fig. 1 Schematic of the configuration studied; the inlet diameter D = 6.35 cm is used to nondimensionalize the length scales.

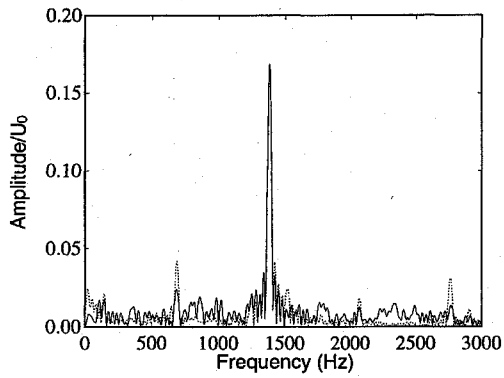

Fig. 2 Fourier spectrum of velocity fluctuations in the shear layer for flow, forced at 5% of inlet pressure at 1380 Hz, 0.24D (1.55 cm) downstream of the combustor step: ——, 120× 240 grid and ·····, 60 × 120 grid.

system and is representative of typical applications. A cylindrical jet with a prescribed mean velocity of $U_0 = 100$ m/s flows through an inlet of diameter D into a cylindrical combustion chamber of larger diameter. An annular exit nozzle at the end of the chamber is modeled to produce choked flow. The choked outflow conditions force the flow to become sonic at the exit throat. At solid walls the normal flux is set to zero and the pressure is extrapolated to the normal stagnation condition. At the inflow, no pressure conditions are set, but the mass flow rate and inflow velocity are specified. The specific flow used in this study is that with an inflow Mach number of 0.31. The physical dimensions are those given in Fig. 1, with the exit consisting of an annular ring at $0.625D$ with an area of 14.89 cm^2. The mass inflow rate is 0.78 kg/s with a mean velocity of 100 m/s, and the initial chamber pressure is 188 kPa.

A fixed computational grid is used with fine zones used near the entrance to the combustor in both the radial and axial directions. The cell sizes gradually increase away from the dump plane. This flow has been shown to be accurately resolved using a 60 × 120 grid.[19,22] For example, at an axial distance of 1.55 cm downstream of the combustor step, the amplitude of velocity fluctuations at the shedding frequency, 1380 Hz, agrees with that of a 120 × 240 grid to within 5% (Fig. 2). Similarly, at a distance of 5.41 cm downstream of the step, the amplitude of the first merging frequency, 690 Hz, agrees to within 1.5% (not shown).

Simulation of Particle Motion

In this study the motion of heavy particles in a one-way coupled system is considered. The particles are assumed to be small in comparison with the smallest scales of the flow, and the loading is such that the presence of the particles does not modify the gas flow in the combustor. Additionally, the presence of a particle does not affect or modify the motion of any neighboring particles. However, the motion of the particles is related directly to the local flow in the ramjet u.

A Lagrangian approach is used to track each particle. Under the assumption that the density of particle ρ_p is much larger than the density of the surrounding fluid ρ_f (a water/air ratio gives $\rho_{\text{water}}/\rho_{\text{air}} \approx 10^3$) the Basset–Boussinesq–Oseen equation of motion[23] reduces to

$$\frac{dV(t)}{dt} = \frac{[u(Y,t) - V(t)]f(Re_p) + W}{\tau_p} \tag{1}$$

$$\frac{dY(t)}{dt} = V(t) \tag{2}$$

Table 1 Relationship between particle diameter d_p, particle response time τ_p, and Stokes number S

d_p, μm	τ_p, s	S
1	3.12×10^{-6}	4.31×10^{-3}
2	1.25×10^{-5}	1.72×10^{-2}
3	2.81×10^{-5}	3.88×10^{-2}
4	5.00×10^{-5}	6.90×10^{-2}
5	7.81×10^{-5}	0.108
6	1.12×10^{-4}	0.155
7	1.53×10^{-4}	0.211
8	2.00×10^{-4}	0.276
9	2.53×10^{-4}	0.349
10	3.12×10^{-4}	0.431
15	7.03×10^{-4}	0.970
20	1.25×10^{-3}	1.72
25	1.95×10^{-3}	2.70
30	2.81×10^{-3}	3.88
50	7.81×10^{-3}	10.7

where $V(t)$ and $Y(t)$ are the velocity and position of the heavy particle. The Stokes response time τ_p and Stokes terminal velocity W are defined as

$$\tau_p = \frac{\rho_p d_p^2}{18\mu} \quad \text{and} \quad W = \tau_p g \tag{3}$$

where ρ_p and d_p are the density and diameter of the sphere and μ the dynamic viscosity of the surrounding fluid. Here we use $\rho_p = \rho_{\text{water}}$ and $\mu = \mu_{\text{air}}$ at one atmosphere of pressure and 288 K, and gravity effects are neglected ($W = 0$). The characteristic flow time is taken to be the vortex shedding frequency at the combustor step $t_f = 1/f$. This time is used to compute the Stokes number $S = \tau_p/t_f$. Stokes numbers for various particle diameters are given in Table 1. The coefficient $f(Re_p)$ is a scalar function of the particle Reynolds number $Re_p = |V - u|d_p/\nu_{\text{air}}$ and is equal to unity for the Stokes flow assumption of this study. The effect of using a nonlinear drag law to calculate $f(Re_p)$ as compared to the linear assumption used here has been studied by Wang and Maxey[2] for heavy particles settling in homogeneous isotropic turbulence. They found small quantitative but no qualitative differences using a nonlinear drag law. Results for the current system under consideration lead to a similar conclusion.[24]

Particles are injected into the ramjet combustor every $10\Delta t$, where $\Delta t = 0.376 \times 10^{-6}$ s, at the corner of the combustor step, $r = D/2$ and $z = 0$, with zero radial velocity and streamwise velocity $v_{\text{inj}} = 50$ m/s. This injection location and velocity were chosen to both maximize dispersion and to model a true fuel injection combustor system. Uthuppan et al.[7] investigated the effect of injection location in a jet and found that dispersion is optimal injecting in the core of the shear layer. We chose an injection velocity of 50 m/s because this is the approximate downstream velocity of the vortex structures. Injecting at this velocity provides the best opportunity for particle interaction with these flow structures. Other injection locations and velocities were examined and indicate that these, indeed, are the optimal injection location and velocity.

A fourth-order Adams–Bashforth method is used to integrate the particle velocity in time and a fourth–order Adams–Moulton method to obtain the particle location. A two-dimensional sixth-order Lagrangian interpolation scheme[25] is used to interpolate flow properties to the particle locations.

Both reflective and absorptive wall boundary conditions have been employed, with an emphasis on the latter. By reflective, we mean that particles that hit a wall are assumed to bounce back into the ramjet combustor in a perfectly elastic manner with purely reflective symmetry (specular reflection). Absorptive boundary conditions are those in which a particle is assumed to stick to the combustor wall upon impact and remain fixed at that location for the remainder of the simulation.

Results

The particular flow configuration just described has been studied in detail by Kailasanath et al.[9] They found that vortex shedding at the

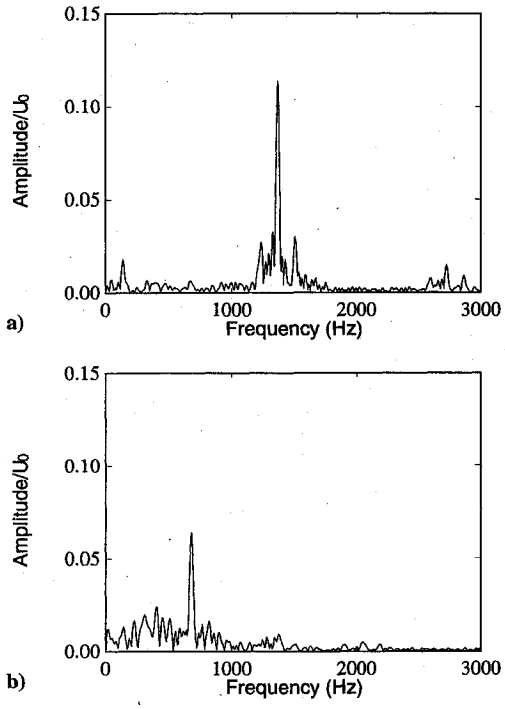

Fig. 3 Fourier spectrum of velocity fluctuations in the shear layer: a) 0.64D (4.1 cm) downstream of the combustor step and b) 1.72D (10.9 cm) downstream of the combustor step.

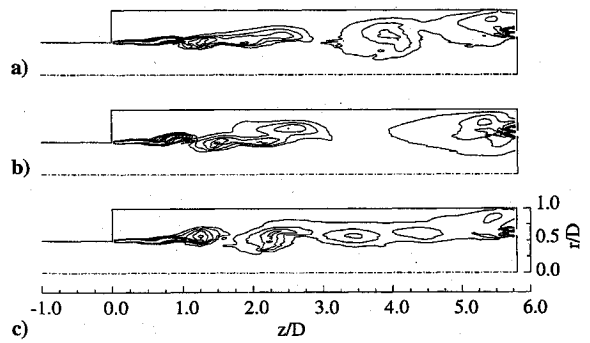

Fig. 4 Lines of constant vorticity inside idealized ramjet combustor at a) $t = 20{,}000\Delta t$ (7.52 ms), b) $t = 40{,}000\Delta t$ (15.04 ms), and c) $t = 100{,}000\Delta t$ (37.6 ms).

combustor step occurs at a frequency of $f = 1380$ Hz corresponding to a Strouhal number of $Sr_{\theta_0} = f\theta_0/U_0 = 0.0146$, where $\theta_0 = 0.106$ cm is the initial shear layer thickness defined by the computational grid.[9] A Fourier analysis of velocity fluctuations at a distance of 0.64D from the dump plane confirms this finding (Fig. 3a). Analysis at 1.72D indicates a second characteristic frequency of 690 Hz $Sr_{\theta_0} = 0.0073$, the first subharmonic of the vortex shedding frequency (Fig. 3b). Finally, we note other geometry related frequencies that may come into play. These include the quarter wave of the inlet (145 Hz), the first longitudinal mode frequency of the combustor (445 Hz), and a beat frequency between the inlet and combustor frequencies (300 Hz). Typical vorticity contours of this flow at various times can be seen in Fig. 4. Here only the upper half-plane is shown.

The results presented here are mainly from simulations with absorptive boundary conditions. Except where noted, the results for simulations with specular reflective boundary conditions yield qualitatively similar results.

Figures 5–7 show particle positions for various particle sizes at times corresponding to the flow shown in Fig. 4. It is fairly evident that small particles remain in the shear layer and are transported with the large vortex structures. Conversely, at intermediate particle sizes [$S \approx \mathcal{O}(1)$ or $d_p \approx 15\,\mu$m] the formation of particle sheets can clearly be seen outside of and between areas of high vorticity.

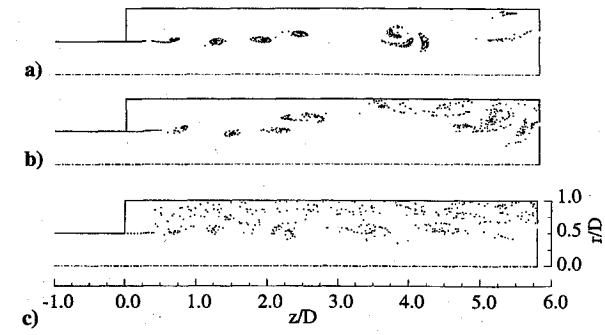

Fig. 5 Particle locations inside idealized ramjet combustor for 1-μm-diam particles (S = 0.004) at a) $t = 20{,}000\Delta t$ (7.52 ms), b) $t = 40{,}000\Delta t$ (15.04 ms), and c) $t = 100{,}000\Delta t$ (37.6 cms).

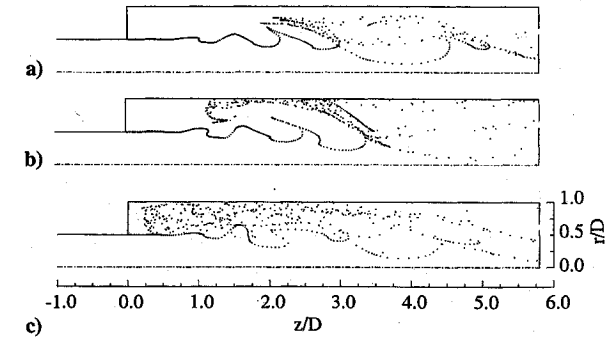

Fig. 6 Particle locations inside idealized ramjet combustor for 15-μm-diam particles (S = 0.970) at a) $t = 20{,}000\Delta t$ (7.52 ms), b) $t = 40{,}000\Delta t$ (15.04 ms), and c) $t = 100{,}000\Delta t$ (37.6 ms).

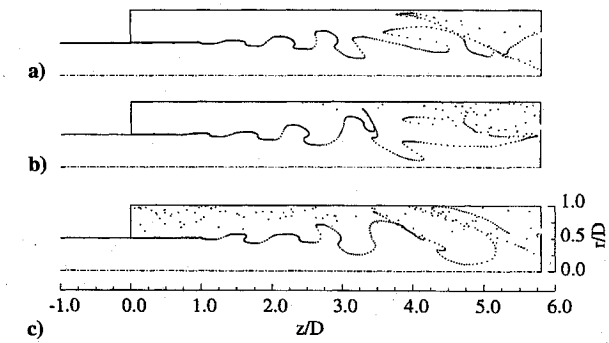

Fig. 7 Particle locations inside idealized ramjet combustor for 30-μm-diam particles (S = 3.881) at a) $t = 20{,}000\Delta t$ (7.52 ms), b) $t = 40{,}000\Delta t$ (15.04 ms), and c) $t = 100{,}000\Delta t$ (37.6 ms).

Particle Dispersion

Figure 8 shows the time-averaged dispersion $\overline{\delta(t)}$ of all particles in the combustor. The dispersion $\delta(t)$, in centimeters, is defined by

$$\delta(t) = \left[\frac{\sum_{i=1}^{N(t)}(r_i(t) - r_{io})^2}{N(t)}\right]^{\frac{1}{2}} \tag{4}$$

where $r_{io} = 3.175$ cm = injection location and $N(t)$ is the number of particles in the combustor at time t. The quantity $\overline{\delta(t)}$ is obtained by averaging collected sets of data from a simulation run. Our results indicate that after an extended period of time the dispersion, initially increasing with time, eventually settles to a quasisteady state. For the Stokes numbers used in this study, this time is on the order of 0.015 s, or approximately 40,000 time steps, corresponding to approximately 21 vortex shedding events. Therefore, to obtain accurate values for the well-mixed system, we do not begin to sample particle dispersion data used to obtain $\overline{\delta(t)}$ until $t = 0.02256$ s, or 60,000 time steps after particle injection has begun. This sampling continues until the end of the simulation run, in this case an additional 200,000 steps or 0.0752 s. Included in Fig. 8 are data that includes particles that have

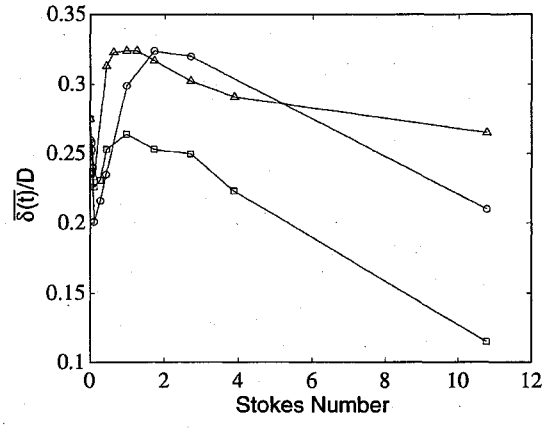

Fig. 8 Time-averaged dispersion as a function of Stokes number for absorptive boundary conditions including particles that have stuck to the combustor wall (○), for absorptive boundary conditions excluding particles that have contacted the combustor wall (□), and for specular reflecting boundary conditions (△).

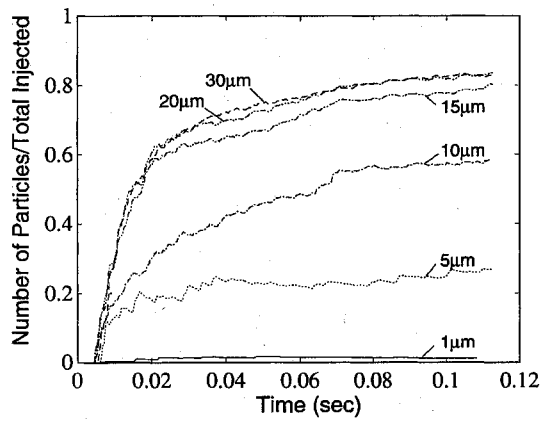

Fig. 9 Number of particles deposited on combustor walls vs time.

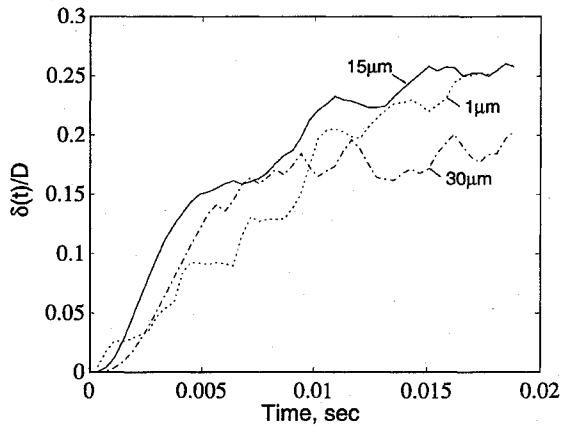

Fig. 10 Dispersion vs time for 1-, 15- and 30-μm-diam particles (S = 0.004, 0.970, and 3.881).

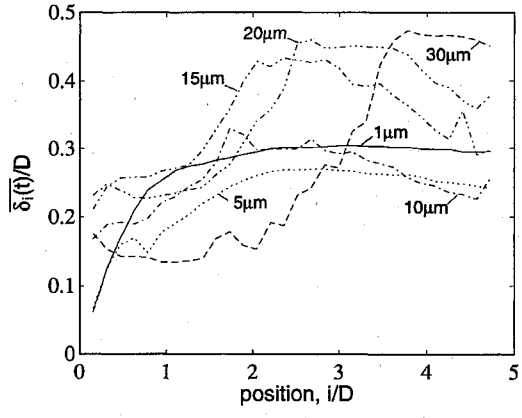

Fig. 11 Time-averaged local dispersion $\overline{\delta_i(t)}/D$, where i is the downstream distance from the combustor step in centimeter.

stuck to, or been deposited on, combustor walls as well as dispersion values that do not include such particles.

Discounting small particle behavior, dispersion is maximized at $d_p = 15\ \mu$m ($S = 0.970$) if deposited particles are not included. When included, dispersion is maximized at a higher particle diameters. This is because particles deposited on the outer radial walls will increase the dispersion measurement. Figure 9 shows that the number of deposited particles continues to increase with particle diameter until $d_p = 20\ \mu$m ($S = 1.725$), the point at which dispersion is maximized.

That the time-averaged dispersion is high for small particles does not necessarily mean that dispersion is optimal in this regime. Figure 10 clearly demonstrates that the initial, time-dependent dispersion can be higher for other particle sizes. The high time-averaged dispersion for small particles is an artifact resulting from a backflow region along the outer combustor wall. Particles that are carried to the end of the combustor and do not exit through the nozzle are transported in this backflow region. Therefore, any particles inside the combustor but not inside the shear layer are at or near the maximum radial distance defined by the confining geometry creating a higher measured dispersion. This is a deceptive feature directly resulting from the confining walls; high dispersion for small particles is not because of ejection from the shear layer but because of fluid transport of particles that do not exit the shear layer and are carried in the backflow near the outer combustor wall. We note that at the end of a typical simulation run for $d_p < 5\ \mu$m the number of particles that exit the combustor will have reached a total on the order of 70% of total particles injected. While increasing with time, this total will never reach 100% for a system with continuous injection because of a finite particle residence time inside the combustor.

Also seen in Fig. 8 is the time-averaged dispersion with specular reflecting boundary conditions. Dispersion reaches a peak at particle diameters near $d_p = 15\ \mu$m or $S = 0.970$. The relatively higher overall dispersion is because of the accumulation of particles near the outer radial wall. In the preceding case, it was seen that a large number of particles made contact with the outer wall. Now, instead of remaining on the wall, these particles are deflected back into the flow and congregate in the low-vorticity regions adjacent to walls.

To evaluate particle dispersion in different regions of the combustor, we define a second dispersion function $\delta_i(t)$, which measures the dispersion via Eq. (4) for particles in the region i cm $< z <$ (i + 1) cm. Thus, $\delta_1(t)$ is the dispersion at time t for all particles 1–2 cm downstream of the injection location. Figure 11 shows $\delta_i(t)$ averaged over time for 250,000Δt, sampled every 50Δt and $i = 1, \ldots, 30$. For very small particles ($S \ll 1$) the dispersion is quite uniform; however, for intermediate-sized particles there is a definite bias indicating areas of higher dispersion. This is because of the tendency of intermediate sized particles to migrate out of the shear layer, away from regions of intense vorticity. Particles that are ejected toward the combustor wall accumulate at nearby low-vorticity areas. As the particle size increases, it takes longer for them to exit the shear layer region and the maximum in the dispersion distribution moves downstream. Note that although 15-μm-diam particles ($S = 0.97$) exhibit the highest global dispersion, as seen in Figs. 8 and 10, here it can be seen that higher dispersion is obtainable at different axial locations for different particle sizes.

Figure 6 indicates that at intermediate Stokes numbers all particles are not carried downstream. To quantify streamwise particle distribution the following method was adopted. A function $P_i(t)$ is defined as the fraction of particles in the interval i cm $< z <$ (i+1) cm of the total number of particles in the interval 1 cm $< z <$ 31 cm for $i = 1, \ldots, 30$. For a given time t, $P_i(t)$ gives the distribution of particles in the streamwise direction. Figure 12 shows the time average of $P_i(t)$ and indicates that for intermediate to large sized particles there exists a streamwise distance at which

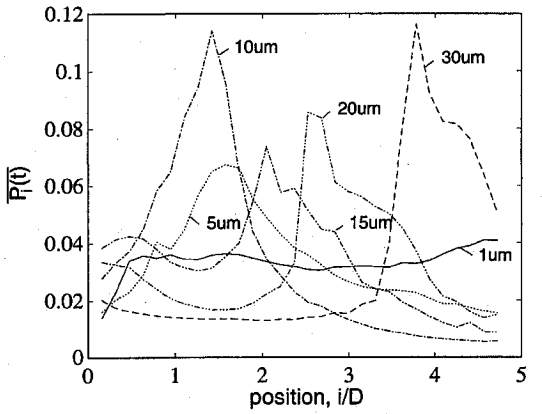

Fig. 12 Time-averaged particle distribution $\overline{P_i(t)}$, where i is the downstream distance from the combustor step in centimeter.

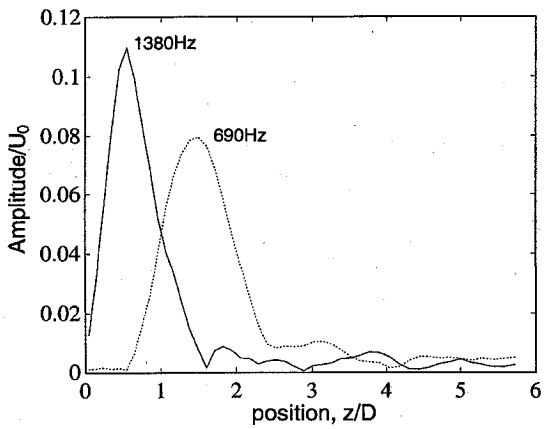

Fig. 13 Amplitude of 1380- and 690-Hz components of velocity fluctuations in the shear layer vs axial distance downstream.

particles tend to accumulate. As with the dispersion distribution, this distance moves downstream as the particle size is increased.

Figure 13 shows the amplitude of the shedding and merging components of the flow velocity in the shear layer vs downstream distance. It is clear that particle motion should be characterized by the shedding frequency near the injection location ($z = 0$). The merging frequency does not become dominant until $z \approx D$ and is much lower in amplitude. For intermediate to high particle response times, a shift to this characteristic frequency will not occur until particles are well into the combustor and noise dominates the signal. It is expected, therefore, that dispersion would most likely be characterized by the shedding frequency throughout much of the combustor except at very low Stokes numbers, in which case the particles respond immediately to the surrounding fluid.

The data used to construct $\delta_i(t)$ and $P_i(t)$ can be used to determine whether there is any correlation between particle dispersion and time-dependent flow structures and acoustics. Taking a Fourier transform of $D_i(t)$ and $P_i(t)$ will indicate any characteristic frequencies. Figures 14a–14c show the Fourier spectra of $\delta_4(t)$, $\delta_{10}(t)$, and $\delta_{20}(t)$ for 15-μm-diam particles ($S = 0.97$). Previously it was established that the dominant frequencies at these locations were the frequency due to vortex shedding, 1380 Hz, and the first vortex merging frequency, 690 Hz. Other than some inconsequential low-frequency noise, it is seen that it is the shedding frequency that governs the behavior of dispersion for intermediate sized particles, even at downstream locations where the merging frequency governs the fluid flow. This property is observed for all particle sizes studied except for cases at very low Stokes numbers where the merging frequency and associated harmonics are seen. This is an expected result as the particle response time for all but the smallest particles is large enough to suggest that characteristic flow frequencies at one location will not be observed in characteristic particle quantities until

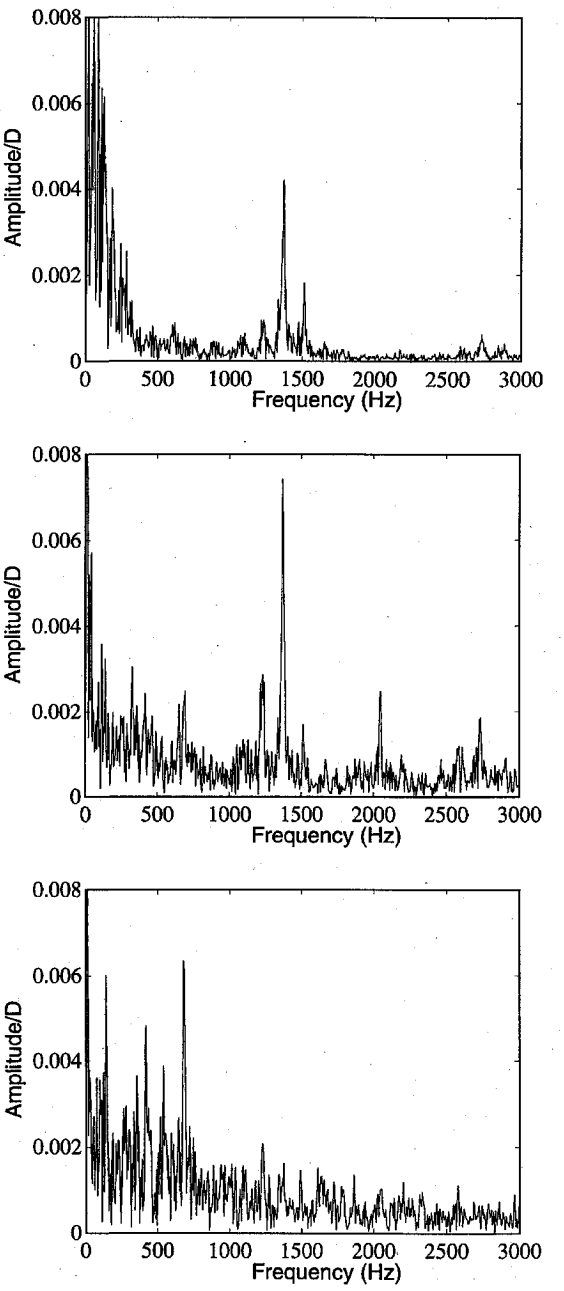

Fig. 14 Fourier spectra of local particle dispersion: a) 0.63D (4.0 cm) downstream of the combustor step, b) 1.57D (10.0 cm) downstream of the combustor step, and c) 3.15D (20 cm) downstream of the combustor step for $S = 0.970$ ($d_p = 15$ μm).

farther downstream. Similarly, the merging frequency, 690 Hz, is not seen in the dispersion spectra until well downstream of the first vortex merging. This also explains the lack of correlation with any of the acoustic modes of the system. For the parameters of the system studied here, it is the second and subsequent mergings in the shear layer that are affected by the acoustics. Based on the results discussed, these frequencies will be expected to affect the dispersion only at locations farther downstream than the second merging. By then, however, the end of the combustor is reached and most of the particles have also been already dispersed. The vortical structures have also grown to nearly reach the wall of the combustor. Therefore, the particle dispersion at none of the locations studied is dominated by the system acoustic frequencies. A wider diameter and longer combustor might allow some additional unimpeded growth of the shear layer and have locations where the acoustic frequencies of the system are observed. However, the acoustic frequencies themselves will be lower in a wider and longer system. Hence, further studies are needed to more definitely conclude on the effects of system acoustics on dispersion.

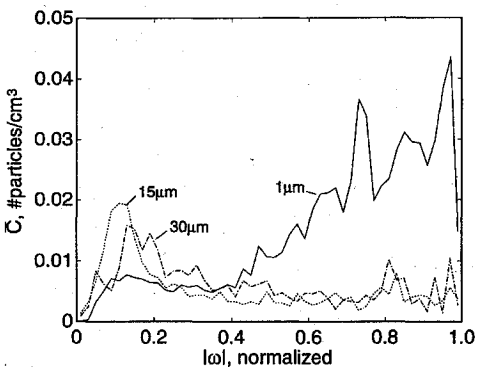

Fig. 15 Time-averaged particle concentration $\bar{C}$ as a function of normalized flow vorticity.

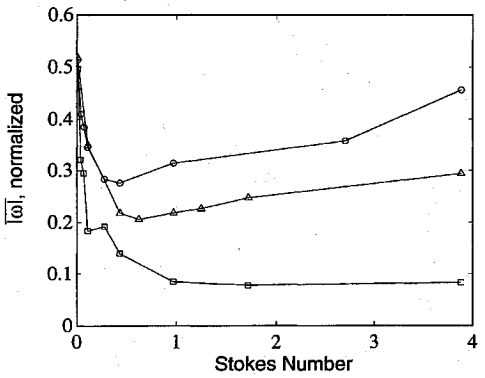

Fig. 16 Dependence of normalized flow vorticity $|\bar{\omega}|$ on Stokes number for absorptive boundary conditions excluding particles that have been deposited on the combustor walls (○), for absorptive boundary conditions including particles that have been deposited on the combustor walls (□), and for specular reflecting boundary conditions (△); zero vorticity is assumed for particles deposited on combustor walls.

Particle Accumulation and Concentration

It has been established that in flows with unconfined boundaries heavy particles with small Stokes numbers tend to accumulate in areas with high flow vorticity, whereas those with Stokes number near unity tend to accumulate in sheets outside such areas.[4,8] To determine a relationship between particle size and flow vorticity, a correlation function $C(t)$ is obtained by dividing the flow domain into equally sized boxes and counting the number of particles in each box. Associated with each box is the magnitude of the flow vorticity at the center of that box. The range spanned by the minimum and maximum of these vorticity values is then divided into evenly spaced intervals and the average number of particles in each box associated with a given interval of vorticity as a fraction of the total number of particles in the system per unit volume is determined. Thus, $C(t)$ gives a measure of particle concentration associated with specific flow vorticity values. Figure 15 shows $C(t)$ averaged over 10 separate data sets of the particle/flowfield for various sized particles plotted against the magnitude of the flow vorticity. For very low Stokes numbers, high concentrations are seen to be correlated with high-vorticity levels. At these low Stokes numbers, particles act essentially as fluid markers. Since particles are injected in the core of the shear layer where vorticity is at its highest, they remain in and are transported by these areas of high vorticity. At intermediate Stokes numbers, relatively higher concentration levels are seen to be associated with low flow vorticity as particles are ejected from the shear layer. At higher Stokes numbers the correlation between low flow vorticity and particle concentration decreases as particle inertia increases, diminishing the effects centrifugal forces have on ejecting particles from the shear layer.

Figure 16 shows the average of the magnitude of the flow vorticity $|\bar{\omega}|$ as a function of Stokes number. Here $|\bar{\omega}|$ is obtained by taking the magnitude of the flow vorticity at each particle location for a given time and averaging over all particles in a given sample and, finally, averaging over 10 samples. It is again seen that low Stokes numbers are associated with high flow vorticity. As the Stokes number increases, a dip is observed where particles accumulate in areas with low vorticity. At higher Stokes numbers, particles become less correlated with flow vorticity and a rise in the curve is seen. This is because of the larger particle inertia and lower dispersion keeping particles within or near the shear layer.

Conclusions

In this study we have found that, as in a free shear layer, particle dispersion is maximized for particle diameters on the order of 15 μm in diameter, or when the Stokes number is near unity, when particles are injected at a velocity on the order of the mean streamwise velocity of flow structures in the combustor. However, this property was found to hold only when particles that have been deposited on the combustor walls are excluded from the dispersion calculation. Including such particles into the dispersion calculation tended to skew these results toward larger diameters. If deposited particles are included, dispersion is not maximized until larger particle diameters because of an increase in particle deposition rate with Stokes number that peaks at $d_p \approx 20\,\mu$m ($S = 1.72$). Lying in between is the specular reflection case in which dispersion was found to reach a maximum at $d_p \approx 15\,\mu$m, or Stokes number near unity, but remain high for larger particles. Here, particles, which have contacted the outer combustor wall, remain in the low-vorticity regions near the outer combustor wall increasing the measured dispersion. These results bring out the role of different wall boundary conditions and suggest the need for further studies involving more complex wall boundary conditions.

Further investigation indicates that whereas global dispersion is optimal for $d_p \approx 15\,\mu$m, local dispersion can be optimal for other sized particles. For the particle sizes considered in this study, our results show that higher local dispersion can be associated with both a farther downstream distance from the injection location and larger particle sizes. In fact, we found that the maximum local dispersion for larger particles can exceed that of the optimal global dispersion. Associated with this increased dispersion with particle size and downstream distance is a more uniform particle distribution. Larger particles, with their higher inertia, travel farther downstream inside the confining geometry; moderately sized particles, while exhibiting high dispersion, tend to accumulate toward the front of the combustor as they are ejected from the shear layer and are transported to the front of the combustor by the backflow along the combustor wall. This indicates that a penalty associated with optimal dispersion is poor axial distribution of particles.

A direct correlation between Stokes number and flow vorticity was found. Low Stokes numbers were found to be associated with high vorticity, indicating that small particles are carried with vortex structures throughout the flowfield. Conversely, intermediate Stokes numbers [$S \approx \mathcal{O}(1)$] were associated with low vorticity as particles are ejected from the shear layer and migrate into regions of low vorticity.

It was also found that the dispersion in the front end of the combustor could be characterized by the vortex shedding frequency even in locations where this was not the characteristic frequency of the flow. That is, the dominant frequency of particle dispersion in a particular location did not always correspond to the dominant fluctuating flow frequency at that location. This does not mean that vortex merging has no effect on dispersion. Further investigation showed that the first merging frequency can characterize dispersion, but at distances much farther downstream than the actual merging events. This also explains the absence of the system acoustic frequencies in the Fourier analysis of particle dispersion at various locations within the combustor. For the particular geometry simulated, the system acoustic frequencies primarily influence the second and subsequent vortex mergings, which occur in the latter half of the combustor. To observe their effect on particle dispersion, much longer and wider systems will be needed. However, the acoustic frequencies for such systems will also be different. Therefore, further research on additional system configurations is needed for more definitive conclusions on the influence of system acoustics on particle dispersion.

Acknowledgments

This work has been supported by the Mechanics and Energy Conversion Division of the Office of Naval Research with Gabriel Roy as program officer, the Naval Research Laboratory, and the National Research Council Research Associate Program. A grant of High Performance Computing (HPC) time from the Department of Defense HPC Shared Resource Center, U.S. Army Corps of Engineers Waterways Experiment Station, is also gratefully acknowledged.

References

[1]Squires, K. D., and Eaton, J. K., "Measurements of Particle Dispersion Obtained from Direct Numerical Simulations of Isotropic Turbulence," *Journal of Fluid Mechanics*, Vol. 226, 1991, pp. 1–35.

[2]Wang, L. P., and Maxey, M. R., "Settling Velocity and Concentration Distribution of Heavy Particles in Homogeneous Isotropic Turbulence," *Journal of Fluid Mechanics*, Vol. 256, 1993, pp. 27–68.

[3]Aggarwal, S. K., Chen, G., Yapo, Y. B., Grinstein, F. F., and Kailasanath, K., "Numerical Simulation of Particle Dynamics in Planar Shear Layers," AIAA Paper 92-0107, Jan. 1992.

[4]Lázaro, B. J., and Lasheras, J. C., "Particle Dispersion in the Developing Free Shear Layer. Part I. Unforced Flow," *Journal of Fluid Mechanics*, Vol. 235, 1992, pp. 143–178.

[5]Reeks, M. W., Swailes, D., Hyland, K. E., and McKee, S., "A Unifying Theory for the Deposition of Particles in a Turbulent Boundary Layer," *Gas-Solid Flows*, ASME FED-Vol. 166, American Society of Mechanical Engineers, New York, 1993, pp. 109–112.

[6]Sommerfeld, M., Huber, N., and Wächter, P., "Particle-Wall Collisions: Experimental Studies and Numerical Models," *Gas-Solid Flows*, ASME FED-Vol. 166, American Society of Mechanical Engineers, New York, 1993, pp. 183–192.

[7]Uthuppan, J., Aggarwal, S. K., Grinstein, F. F., and Kailasanath, K., "Particle Dispersion in a Transitional Axisymmetric Jet: A Numerical Simulation," *AIAA Journal*, Vol. 32, No. 10, 1994, pp. 2040–2048.

[8]Longmire, E. K., and Eaton, J. K., "Structure and Control of a Particle-Laden Round Jet," *Journal of Fluid Mechanics*, Vol. 236, 1992, pp. 217–257.

[9]Kailasanath, K., Gardner, J. H., Oran, E. S., and Boris, J. P., "Numerical Simulations of High-Speed Flows in an Axisymmetric Ramjet," AIAA Paper 88-0339, Jan. 1988.

[10]Martin, J. E., and Meiburg, E., "The Accumulation and Dispersion of Heavy Particles in Forced Two-Dimensional Mixing Layers. Part 1: The Fundamental and Subharmonic Cases," *Physics of Fluids*, Vol. 6, No. 3, 1994, pp. 1116–1132.

[11]Crowe, C. T., Gore, R. A., and Troutt, T. R., "Particle Dispersion by Coherent Structures in Free Shear Flows," *Particulate Science and Technology*, Vol. 3, 1985, pp. 149–158.

[12]Lázaro, B. J., and Lasheras, J. C., "Particle Dispersion in the Developing Free Shear Layer. Part 2. Forced Flow," *Journal of Fluid Mechanics*, Vol. 235, 1992, pp. 179–221.

[13]Lázaro, B. J., and Lasheras, J. C., "Particle Dispersion in a Turbulent, Plane, Free Shear Layer," *Physics of Fluids A*, Vol. 1, No. 6, 1989, pp. 1035–1044.

[14]Chung, J. N., and Troutt, T. R., "Simulation of Particle Dispersion in an Axisymmetric Jet," *Journal of Fluid Mechanics*, Vol. 186, 1988, pp. 199–222.

[15]Crowe, C. T., Chung, J. N., and Troutt, T. R., "Particle Dispersion by Organized Turbulent Structures," *Particulate Two-Phase Flow*, edited by M. C. Roco, Butterworth–Heinemann, Stoneham, MA, 1993, Chap. 18.

[16]Eaton, J. K., and Fessler, J. R., "Preferential Concentration of Particles by Turbulence," *International Journal of Multiphase Flow*, Vol. 20, 1994, pp. 169–209.

[17]Boris, J. P., and Book, D. L., "Solution of Continuity Equation by the Method of Flux Corrected Transport," *Methods in Computational Physics*, Vol. 16, Academic, New York, 1976, pp. 85–129.

[18]Boris, J. P., Grinstein, F. F., Oran, E. S., and Kolbe, R. L., "New Insights into Large Eddy Simulation," *Fluid Dynamics Research*, Vol. 10, 1992, pp. 199–228.

[19]Kailasanath, K., Gardner, J. H., Oran, E. S., and Boris, J. P., "Acoustic-Vortex Interactions in an Idealized Ramjet Combustor," *Proceedings of the 22nd JANNAF Combustion Meeting* (Pasadena, CA), Chemical Propulsion Information Agency Publication 432, Vol. 1, 1985, pp. 341–350.

[20]Kailasanath, K., Gardner, J. H., Oran, E. S., and Boris, J. P., "Numerical Simulations of Acoustic-Vortex Interactions in a Central Dump Ramjet Combustor," *Journal of Propulsion and Power*, Vol. 3, No. 6, 1987, pp. 525–533.

[21]Kailasanath, K., Gardner, J. H., Boris, J. P., and Oran, E. S., "Acoustic-Vortex Interactions and Low-Frequency Oscillations in Axisymmetric Combustors," *Journal of Propulsion and Power*, Vol. 5, No. 2, 1989, pp. 165–171.

[22]Kailasanath, K., Gardner, J. H., Oran, E. S., and Boris, J. P., "Numerical Simulations of the Flowfield in a Central-Dump Ramjet Combustor-I. Tests of the Model and Effects of Forcing," U.S. Naval Research Lab., NRL Memorandum Rept. 5832, Washington, DC, July 1986.

[23]Maxey, M. R., and Riley, J. J., "Equation of Motion for a Small Rigid Sphere in a Nonuniform Flow," *Physics of Fluids*, Vol. 26, No. 4, 1983, pp. 883–889.

[24]Chang, E. J., Kailasanath, K., and Aggarwal, S., "Compressible Flows of Gas-Particle Systems in an Axisymmetric Ramjet Combustor," AIAA Paper 95-2561, July 1995.

[25]Balachandar, S., and Maxey, M. R., "Methods for Evaluating Fluid Velocities in Spectral Simulations of Turbulence," *Journal of Computational Physics*, Vol. 83, No. 1, 1989, pp. 96–125.